

FREQUENCY DOMAIN GPR SIGNAL FORWARD AND INVERSE MODELLING FOR IDENTIFYING THE SUBSURFACE DIELECTRIC PROPERTIES

Sebastien Lambot^{1,3}, Idesbald van den Bosch² and Evert C. Slob³

1. Department of Environmental Sciences and Land Use Planning, Catholic University of Louvain, Belgium; [s.lambot\(at\)CiTG.TUdelft.nl](mailto:s.lambot(at)CiTG.TUdelft.nl)
2. Microwave Laboratory, Catholic University of Louvain, Belgium
3. Department of Geotechnology, Delft University of Technology, The Netherlands

ABSTRACT

Research has focused on the development of a new integrated approach including ground penetrating radar (GPR) design, GPR signal forward modelling, and GPR signal inversion to estimate the dielectric permittivity and electric conductivity of the shallow subsurface. We propose to use an ultrawide band (UWB) stepped frequency continuous wave (SFCW) radar combined with an off-ground monostatic transverse electromagnetic (TEM) horn antenna. Forward modelling is based on linear system response functions for describing the antenna, and on the exact solution of Maxwell's equations for wave propagation in a horizontally multilayered medium representing the subsurface. Model inversion, formulated by the classical least-squares problem, is carried out iteratively using advanced global optimisation techniques. The proposed approach is validated under laboratory conditions on a homogeneous sand subject to different water contents. The frequency dependence of the electric conductivity is characterized and the effect of soil roughness is analysed. The approach offers great promise in bridging the gap between airborne/spaceborne measurements of surface soil moisture and ground truth measurements.

Keywords: Ground penetrating radar, inverse modelling, soil dielectric properties

INTRODUCTION

The knowledge of soil water dynamics is essential in agricultural and environmental engineering as it controls plant growth, hydrological processes, and the contamination of surface and subsurface water. It has become evident that modelling detailed spatial distributions of water and solutes in the heterogeneous subsurface requires extensive site characterization (1). Characterizing this variability with conventional methods is invasive and thus, time-consuming, costly, and subject to a large degree of uncertainty due to the lack of densely sampled *in situ* measurements.

GPR can be used for non-destructive characterization of the hydrogeophysical properties of the subsurface. However, notwithstanding considerable research has been devoted to GPR, its use for quantitatively assessing the subsurface properties is still constrained by the lack of appropriate GPR techniques. GPR has been used to identify soil stratigraphy (2), to locate water table (3), to follow wetting front movement (4), to measure soil water content (5;6;7,8) to assist in subsurface hydraulic parameter identification (9), to assess soil salinity (10), and also to support the monitoring of contaminants (11). An excellent review on GPR methods for measuring soil water content is given in (12).

The main limitations of the existing GPR characterization methods arise from the strongly simplifying assumptions with respect to the antennas radiative properties and electromagnetic wave propagation phenomena. As a result, only a part of the information contained in the GPR signal is utilized, usually the propagation time. Additionally, commercially available GPR systems have generally a bandwidth less than 1 GHz. A larger bandwidth is needed for a better spatial resolution (13). To circumvent the limitation of the existing methods, (14,15) recently proposed a new promising integrated approach relying on full wave inverse modelling. It is based on a UWB SFCW radar combined with an off-ground monostatic antenna. This radar configuration enables high mobility,

more information to be acquired from the ground owing to the large bandwidth, and further a realistic, accurate, and efficient forward and inverse modeling of the radar signal. The radar-antenna-subsurface system is modeled using linear system transfer functions and the exact solution of the three-dimensional Maxwell's equations for wave propagation in a horizontally multilayered medium. The inversion to identify the subsurface properties is formulated by the classical least squares problem and is carried out iteratively using the global multilevel coordinate search optimization algorithm combined sequentially with the local Nelder-Mead simplex algorithm (16,17).

This paper summarizes the overall approach and extends the previous work by characterizing the frequency dependence of the electric conductivity and analysing the effect of soil roughness on the estimated parameters.

GROUND PENETRATING RADAR SYSTEM

The approach is based on a UWB SFCW radar emulated using a vector network analyzer (VNA) (ZVRE, Rohde & Schwarz) and combined with a linear polarized double ridged broadband TEM horn antenna (BBHA 9120 D, Schwarzbeck Mess-Elektronik) used off the ground in monostatic mode. The signal-to-noise ratio of SFCW radars is better than for time domain systems, since the mean radiated power is much higher (13). The focused beaming of the TEM horn yields high horizontal resolution and permits us to operate with the target situated in the far-field of the antenna. This results in important forward modelling simplifications, as shown in the following section.

FORWARD MODELLING

Antenna equation in the frequency domain

Assuming that the soil surface is in the Fraunhofer region (far-field) of the antenna, the antenna can be modeled accurately as a point source and receiver (18). Moreover, given the monostatic configuration, antenna modeling does not require the knowledge of the source radiation pattern, since the picked up signal has only propagated along the antenna axial direction. Consequently, the antenna being a causal time-invariant linear system, it can be modeled as a simple linear system composed of elementary model components in series and parallel, all of which are characterized by an own frequency response function accounting for a specific electromagnetic phenomenon. The antenna is modeled using the block diagram represented in Figure 1. The resulting transfer function, expressed in the frequency domain, is given by:

$$S_{11}(\omega) = \frac{Y(\omega)}{X(\omega)} = H_i(\omega) + \frac{H_t(\omega)G_{xx}^\uparrow(\omega)H_r(\omega)}{1 - H_f(\omega)G_{xx}^\uparrow(\omega)} \quad (1)$$

where $S_{11}(\omega)$ is the quantity measured by the VNA; $Y(\omega)$ and $X(\omega)$ are the received and emitted signals at the VNA reference plane, respectively; $H_i(\omega)$, $H_t(\omega)$, $H_r(\omega)$, and $H_f(\omega)$ are the complex return loss, transmitting, receiving, and feedback loss transfer functions of the antenna, respectively; $G_{xx}^\uparrow(\omega)$ is the transfer function of the air-subsurface system modelled as a multilayered medium; and ω is the angular frequency.

Subsurface model

Given the monostatic configuration and the focused beaming of the antenna, the measured radar signal has mainly propagated in the vertical axial direction. As a result, the horizontal variability of the dielectric properties inherently encountered in environmental systems is expected to play a negligible role, and the ground can be modeled realistically and efficiently using a horizontally multilayered configuration, as depicted in Figure 2. The model is three-dimensional and consists of N horizontal layers separated by $N-1$ interfaces. The medium of the n^{th} layer is homogeneous and characterized by the dielectric permittivity ϵ_n , electric conductivity σ_n , and thickness h_n . The magnetic permeability is assumed to be equal to the permeability of free space. The source and receiver point is located in the upper half-space, representing the air layer. The emitting part of the

TEM horn is approximated by an infinitesimal horizontal x-directed electric dipole, whereas the receiving part of the antenna is emulated by recording the horizontal x-directed component of the backscattered (upward) electric field.

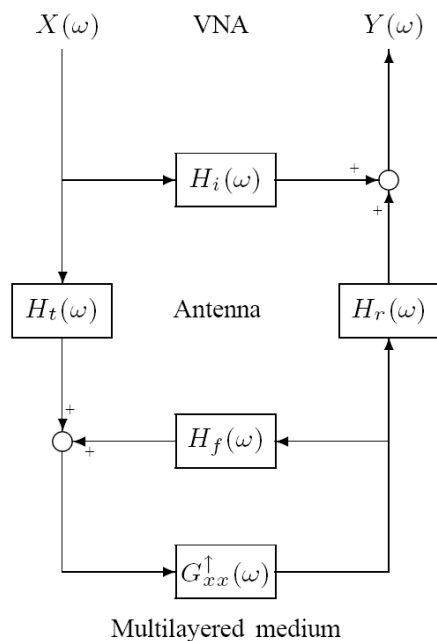


Figure 1: Block diagram representing the VNA-antenna-multilayered medium system modeled as linear systems in series and parallel.

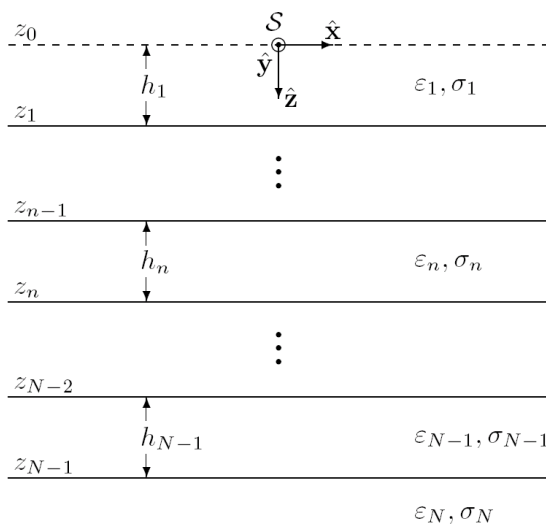


Figure 2: Model configuration: three-dimensional N-layered medium with a point source S.

For this configuration, closed form analytical expressions can be derived for the exact solution of the system of Maxwell's equations. Following the approach of (19), we compute the air-subsurface transfer Green function $G_{xx}^{\uparrow}(\omega)$, i.e., the solution of Maxwell's equations, by computing recursively the transverse electric and magnetic global reflection coefficients of the multilayered system in the two-dimensional spatial Fourier domain. It is worth noting that the three-dimensional model is essential to account for spherical divergence in electromagnetic wave propagation.

MODEL INVERSION

In the particular case where no prior information on the parameters is taken into account and assuming observation errors to be normally distributed with mean zero and covariance matrix \mathbf{C} , in-

dependent, and homoscedastic, the maximum likelihood theory reduces to the weighted least-squares problem. The objective function to be minimized is accordingly defined as follows:

$$\Phi(\mathbf{b}) = \left| \mathbf{G}_{xx}^{\uparrow*}(\omega) - \mathbf{G}_{xx}^{\uparrow}(\omega, \mathbf{b}) \right|^T \mathbf{C}^{-1} \left| \mathbf{G}_{xx}^{\uparrow*}(\omega) - \mathbf{G}_{xx}^{\uparrow}(\omega, \mathbf{b}) \right| \quad (2)$$

where $\mathbf{G}_{xx}^{\uparrow*}(\omega)$ and $\mathbf{G}_{xx}^{\uparrow}(\omega, \mathbf{b})$ are the vectors containing the observed and simulated response functions, respectively. Since these response functions are complex functions, the difference between observed and modelled data is expressed by the amplitude of the errors in the complex plane. As in most electromagnetic inverse problems, this function is highly nonlinear and is characterized by an oscillatory behaviour and a multitude of local minima. This complex topography necessitates the use of a robust global optimisation algorithm. We use the global multilevel coordinate search algorithm (16) combined sequentially with the classical Nelder-Mead simplex algorithm (17).

LABORATORY EXPERIMENTS

Experimental setup

Radar measurements were carried out under controlled laboratory conditions on a tank filled with a two-layered sand. The water content of the bottom layer was fixed, whereas the top layer was subject to nine different water contents. The thickness of each layer was equal to about 13 cm. A horizontal metal sheet was installed to control the bottom boundary conditions in the electromagnetic model. Indeed, laboratory materials underneath this metal sheet have no influence on the measured backscattered signal. The antenna was situated at about 40 cm above the sand surface. Parameter $S_{11}(\omega)$ was measured sequentially over the range 1-2 GHz with a frequency step of 8 MHz.

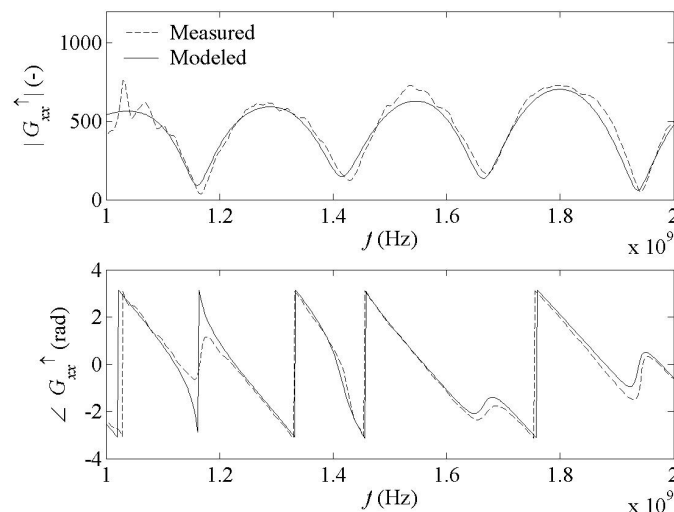


Figure 3: Measured and modeled Green's function for a two-layered sandy soil.

Estimation of the dielectric permittivity

Figure 3 shows the measured and modeled complex Green's function for water content $\theta = 0.04$. Although wave propagation phenomena are relatively complex in this configuration, the observed Green's function is remarkably well reproduced by the conceptual forward model. Figure 4 represents the inversely estimated relative dielectric permittivity as a function of the different water contents. We can observe that inverse estimations are very consistent with the different water contents. Fitting a third order polynomial to the data led to a standard deviation of 0.0070 for the error on the predicted water content, which is very satisfying. The difference between time domain reflectometry (TDR) and GPR is to be attributed to the difference in the operating frequencies and also to the different characterization scales.

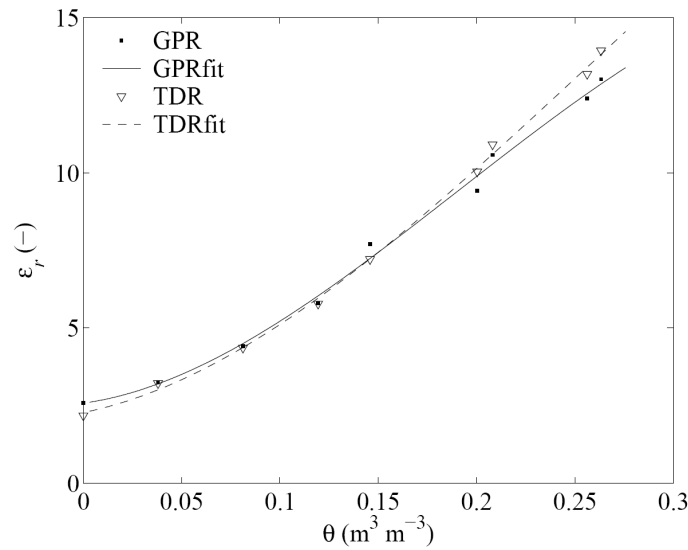


Figure 4: Inversely estimated relative dielectric permittivity (ϵ_r) as a function of different water contents (θ). GPR derived data (square symbols) are compared to TDR measurements (triangular symbols).

Frequency dependence of the electric conductivity

Figure 5 represents the inversely estimated electric conductivity as a function of frequency for three different water contents. Inversions were performed in five different frequency ranges, between 1 and 3 GHz. The dielectric permittivity was assumed to be independent of frequency. We can observe, as expected, that the electric conductivity increases with water content (dielectric permittivity) and also increases significantly with frequency. The values of the electric conductivity are not always consistent with the water content level, which may be attributed to the variation of sand density between the different water contents.

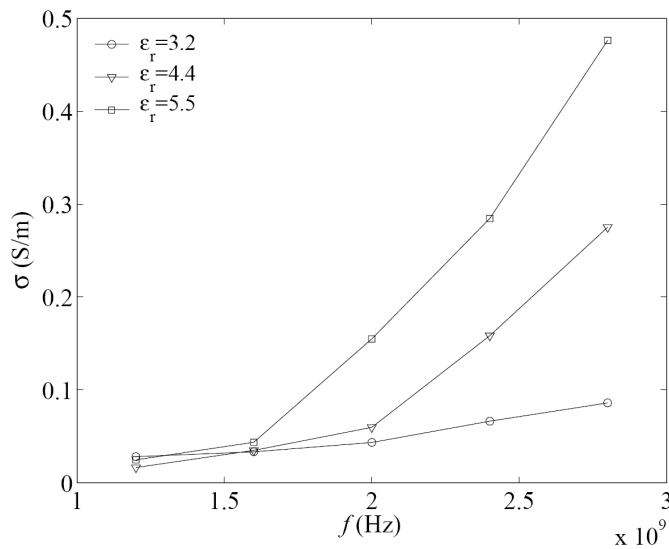


Figure 5: Inversely estimated electric conductivity as a function of frequency and different permittivities (water contents).

Effect of soil roughness

The effect of soil roughness was investigated by setting a one-layered sand subject to different roughness and water contents. Surface roughness is quantified using the standard deviation of the elevations (s_h). Figure 6 represents the inversely estimated dielectric permittivity as a function of surface roughness. We observe that for the frequency range 1-2 GHz, surface roughness has a

small effect on the estimation when $s_h < 0.6$ cm. Lower frequencies would be required to make the assumption of a flat earth valid when dealing with more important roughness.

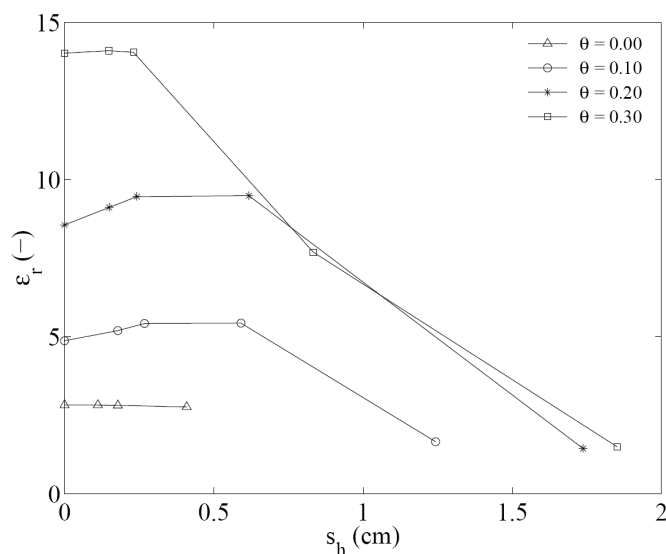


Figure 6. Inversely estimated relative dielectric permittivity as a function of roughness and water content.

CONCLUSIONS

We describe a new integrated radar/signal analysis method which is promising for the real time mapping of the soil electric properties. The overall approach is successfully validated under laboratory conditions. The most important result of the reported study is that we have a purely conceptual model which emulates remarkably well the radar-antenna-subsurface system. This enables the use of inverse modeling techniques for estimating quantitatively and simultaneously the dielectric permittivity and electric conductivity of the subsurface. The overall approach still needs to be improved and to be validated progressively under conditions closer to the reality before resulting in a field usable prototype. The approach offers great promise in bridging the gap between airborne/spaceborne measurements of surface soil moisture and ground truth measurements.

ACKNOWLEDGMENT

This work was supported by the FRIA, FNRS, Catholic University of Louvain, Royal Military Academy (Belgium), and Delft University of Technology (The Netherlands).

REFERENCES

- 1 Yeh T-C J, L W Gelhar & A L Gutjahr, 1985. Stochastic analysis of unsaturated flow in heterogeneous soils, 1, Statistically isotropic media. Water Resources Research, 21: 447-456
- 2 Davis J L & A P Annan, 1989. Ground penetrating radar for high resolution mapping of soil and rock stratigraphy. Geophysical Prospecting, 37: 531-551
- 3 Nakashima Y, H Zhou & M Sato, 2001. Estimation of groundwater level by GPR in an area with multiple ambiguous reflections. Journal of Applied Geophysics, 47: 241-249
- 4 Vellidis G, M C Smith, D L Thomas & L E Asmussen, 1990. Detecting wetting front movement in a sandy soil with ground penetrating radar. Transactions of the ASAE, 33: 1867-1874

- 5 Chanzy A, A Tarussov, A Judge & F Bonn, 1996. Soil water content determination using digital ground penetrating radar. Soil Science Society of America Journal, 60: 1318-1326
- 6 Weiler K W, T S Steenhuis, J Boll, J & K-J S Kung, 1998. Comparison of ground penetrating radar and time domain reflectometry as soil water sensors. Soil Science Society of America Journal, 62: 1237-1239
- 7 Huisman J A, C Sperl, W Bouten & J M Verstraten, 2001. Soil water content measurements at different scales: accuracy of time domain reflectometry and ground penetrating radar. Journal of Hydrology, 245: 48-58
- 8 Serbin G & D Or, 2003. Near-surface water content measurements using horn antenna radar: methodology and overview. Vadose Zone Journal, 2: 500-510
- 9 Hubbard S S, Y Rubin & E Majer, 1997. Ground-penetrating-radar-assisted saturation and permeability estimation in bimodal systems. Water Resources Research, 33: 971-990
- 10 al Hagrey S A & C Muller, 2000. GPR study of pore water content and salinity in sand. Geophysical Prospecting, 48: 63-85
- 11 Yoder R E, R S Freeland, J T Ammons & L L Leonard, 2001. Mapping agricultural fields with GPR and EMI to identify offsite movement of agrochemicals. Journal of Applied Geophysics, 47: 251-259
- 12 Huisman J A, S S Hubbard, J D Redman & A P Annan, 2003. Measuring soil water content with ground penetrating radar: A review Vadose Zone Journal, 2: 476-491
- 13 Daniels D J, 1996. Surface penetrating radar (The Inst. Electrical Eng., London) 320 pp.
- 14 Lambot S, E C Slob, I van den Bosch, B Stockbroeckx, B Scheers & M Vanclooster, 2004. Estimating soil electric properties from monostatic ground-penetrating radar signal inversion in the frequency domain. Water Resources Research, 40: W04205, doi:10.1029/2003WR002095
- 15 Lambot S, E C Slob, I van den Bosch, B Stockbroeckx & M Vanclooster, 2004. Modeling of ground-penetrating radar for accurate characterization of subsurface electric properties. IEEE Transactions on Geoscience and Remote Sensing, 42, 2555-2568, 2004
- 16 Huyer W & A Neumaier, 1999. Global optimization by multilevel coordinate search. Journal of Global Optimization, 14: 331-355
- 17 Lambot S, M Javaux, F Hupet & M Vanclooster, 2002. A global multilevel coordinate search procedure for estimating the unsaturated soil hydraulic properties. Water Resources Research, 38(11): 1224, doi:10.1029/2001WR001224
- 18 Balanis C A, 1997. Antenna Theory: Analysis and Design (John Wiley & Sons, New York) 950 pp.
- 19 Slob E C & J Fokkema, 2002. Coupling effects of two electric dipoles on an interface. Radio Science, 37: 1073, doi:10.1029/2001RS2529